TNF target flame: Lean premixed turbulent hydrogen-air slot-jet flames at various Reynolds and Karlovitz numbers

Authors

Michael Gauding[a], Lukas Berger[a,b,c], Heinz Pitsch[a]

Affiliations

[a] Institute for Combustion Technology, RWTH Aachen University, Germany

[b] Thermo and Fluid Dynamics (FLOW), Faculty of Engineering, Vrije Universiteit Brussel, Brussels 1050, Belgium

[c] Brussels Institute for Thermal-Fluid Systems and Clean Energy (BRITE), VUB-ULB, Brussels 1050, Belgium

Introduction

Lean premixed hydrogen-air flames are prone to thermodiffusive (TD) instabilities, which originate from an imbalance between species and thermal diffusive fluxes. TD instabilities have a leading order impact on flame dynamics and substantially increase the local reactivity. They interact synergistically with turbulence, as increased curvature and stretch rates further amplify the TD response. The physical mechanisms governing turbulent thermodiffusively unstable flames are not yet fully understood and remain challenging to model. Data from direct numerical simulations (DNS) is well suited to develop and validate models that can be employed in large-eddy simulations (LES) or RANS simulations.

The DNS database presented comprises seven cases of turbulent, lean premixed hydrogen-air jet flames under ambient conditions, covering a broad range of Reynolds and Karlovitz numbers through systematic variations in the slot width and jet velocity.

DNS configuration and methods

The reactive, unsteady Navier-Stokes equations are solved under the low-Mach-number approximation using the inhouse code CIAO [5]. The governing equations are discretized using a semi-implicit finite difference method with Crank-Nicolson time advancement and an iterative predictor-corrector scheme. Spatial and temporal staggering is employed to improve the numerical accuracy.

Second-order finite-difference schemes are used for spatial discretization of the momentum equation and the diffusive terms in the scalar transport equations. Convective terms in the scalar equations are discretized using a fifth-order weighted essentially non-oscillatory (WENO) scheme to ensure bounded solutions. Chemical source terms are treated using symmetric Strang operator splitting.

Chemical kinetics are described by the reaction mechanism of Burke et al. [4], involving nine species. Transport properties, such as thermal conductivity and viscosity, are evaluated using

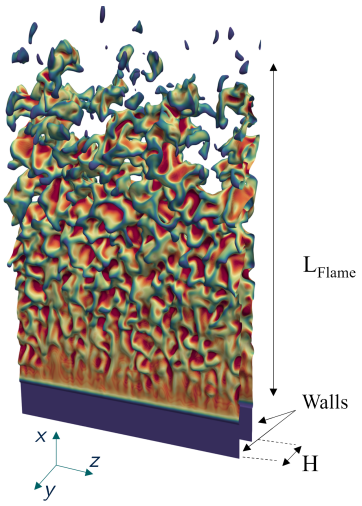

Figure 1: Schematic of the simulation configuration. The flame is represented by an iso-surface of C_{H2} that is colored by the heat release rate.

mixture-averaged formulations. Species diffusion coefficients are computed assuming constant Lewis numbers evaluated in the burnt gas. Thermodiffusion (Soret effect) is included. More details are provided by Berger et al. [1, 2].

The simulation data are stored in the HDF5 format. All simulations were performed on a uniform and equidistant mesh. Depending on the Karlovitz number, the flame thickness l_F is resolved with 10 to 40 grid points. The Kolmogorov length scale η is resolved with at least one grid cell.

All simulations were performed on the SuperMUC supercomputer at the Leibniz Supercomputing Center (LRZ), Germany, consuming approximately 300 million core-hours. The resulting dataset occupies about 1.5 PB of storage.

Operation conditions

A turbulent lean premixed hydrogen-air flame is considered in a slot-flame configuration at ambient conditions (T_u = 298 K and p = 1 atm) and an equivalence ratio of 0.4. Unburnt mixture is injected into the simulation domain through a turbulent planar channel flow with a hot coflow of burnt gas featuring an adiabatic temperature of T_b = 1418 K and a uniform velocity of 15% of the bulk velocity U. For all flames, the laminar unstretched burning velocity and thermal flame thickness are s_L = 0.17 m/s and l_F = 714 μm, respectively. A schematic of the flame configuration is shown in Fig. 1. Periodic boundary are applied in spanwise direction (z) and free-slip boundary conditions are applied in lateral direction (y). The data is statistically stationary and statistically homogeneous in y-direction. Further details on the setup of the simulations are provided by Berger et al. [1, 2].

For a rigorous investigation of the turbulence-flame interaction, the turbulence conditions are systematically varied by adjusting the slot width H and the bulk velocity U. Variations of the slot Reynolds number Re_0 are achieved by increasing H while keeping U constant. With this approach, the integral length scale l_t, which scales with H, increases, whereas the Kolmogorov length scale η remains approximately unchanged. As a consequence, the Karlovitz number remains

Table 1: Simulation parameters. The labels R and K indicate the Reynolds and Karlovitz number variations, respectively.

	R1K1	**R2K1**	**R3K1**	**R1K2**	**R2K2**	**R3K2**	**R2K3**
Slot width H (mm)	4	8	16	2	4	8	2
Bulk velocity U (m/s)	24	24	24	48	48	48	96
Reynolds number Re_0	5 500	11 000	22 000	5 000	11 000	22 000	11 000
Grid resolution Δ (μm)	70	70	70	35	35	35	16
Flame resolution l_F/Δ	10.2	10.2	10.2	20.4	20.4	20.4	44.6
Flame length (mm)	40	57	92	45	56	75	67
Grid size N_x	1024	1792	3456	2176	3264	3840	5376
Grid size N_y	768	1472	2752	1344	2208	3072	3072
Grid size N_z	385	512	1024	384	512	1024	1024

approximately constant despite the increasing Reynolds number. Conversely, the Karlovitz number is increased by halving H and doubling U. This approach keeps the slot Reynolds number Re_0 constant while reducing the Kolmogorov length scale η, thereby increasing Ka.

Exemplary results

Figure 2 visualizes all cases using a two-dimensional slice of the enstrophy field, together with an iso-contour of the progress variable at $C_{\mathrm{H2}} = 0.9$, which indicates the location of maximum heat release. The progress variable is defined as

$$C_{\mathrm{H_2}} = 1 - \frac{Y_{\mathrm{H_2}}}{Y_{\mathrm{H_2,u}}}\,, \tag{1}$$

where $Y_{\mathrm{H_2}}$ denotes the local hydrogen mass fraction and $Y_{\mathrm{H_2,u}}$ the value in the unburnt mixture.

To illustrate the effect of Reynolds on Karlovitz numbers on TD instabilities, Fig. 3 shows the fields of the Bilger mixture fraction Z and the OH mass fraction Y_{OH} for all cases. The Bilger mixture fraction [3] is defined as

$$Z = \frac{Z_{\mathrm{H}} + \nu(Y_{\mathrm{O_2,air}} - Z_{\mathrm{O}})}{1 + \nu Y_{\mathrm{O_2,air}}}\,, \tag{2}$$

where the stoichiometric coefficient ν is defined by the ratio of the molar masses of oxygen and hydrogen as $\nu = 2M_{\mathrm{H_2}}/M_{\mathrm{O_2}}$; $Z_{\mathrm{H_2}}$ and Z_{O} are the element mass fractions of hydrogen and oxygen, receptively and $Y_{\mathrm{O_2,air}}$ is the mass fraction of oxygen in the air. The formation of flame fingers consisting of locally richer and more reactive mixture in positively curved regions is evident under all conditions. These structures are most pronounced for the low Karlovitz number cases and become less distinct at the high Karlovitz numbers. A detailed discussion of the Karlovitz number effect is provided by Berger et al. [2].

In jet flames, the turbulence-flame interaction changes along the streamwise direction. Figure 4

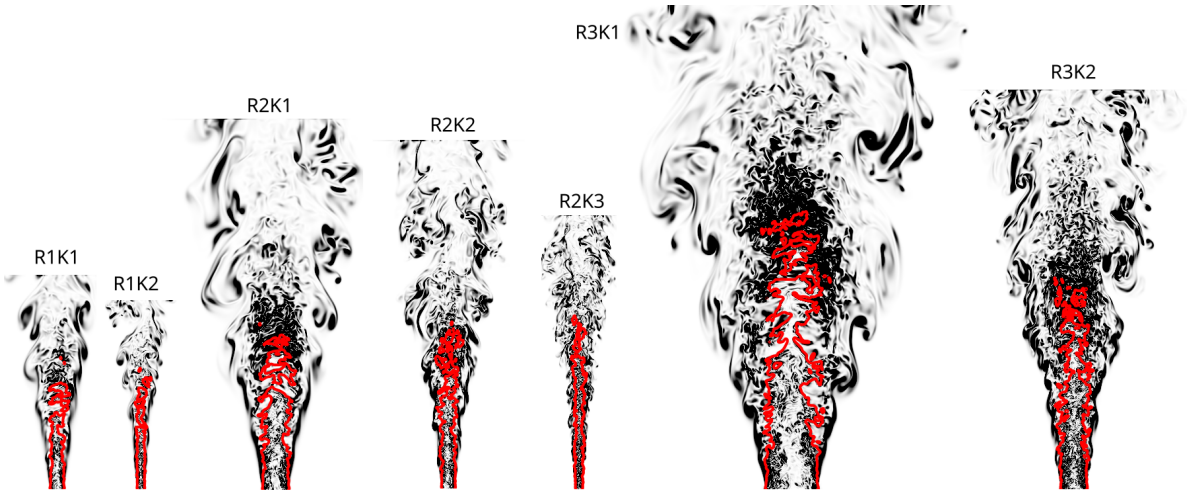

Figure 2: Visualization of the two-dimensional slice of the enstrophy field in the $x - y$ plane for all cases. The iso-contour of $C_{\mathrm{H2}} = 0.9$ is shown by a red line.

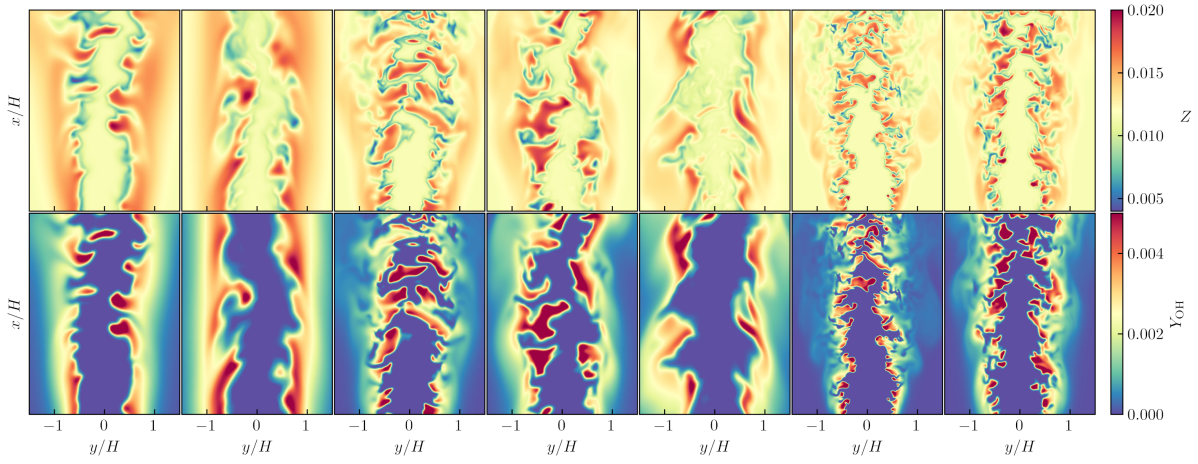

Figure 3: Visualization of the Bilger mixture fraction (top row) and the OH mass fraction (bottom row) for all cases. From left to right: R1K1, R1K2, R2K1, R2K2, R2K3, R3K1, R3K2.

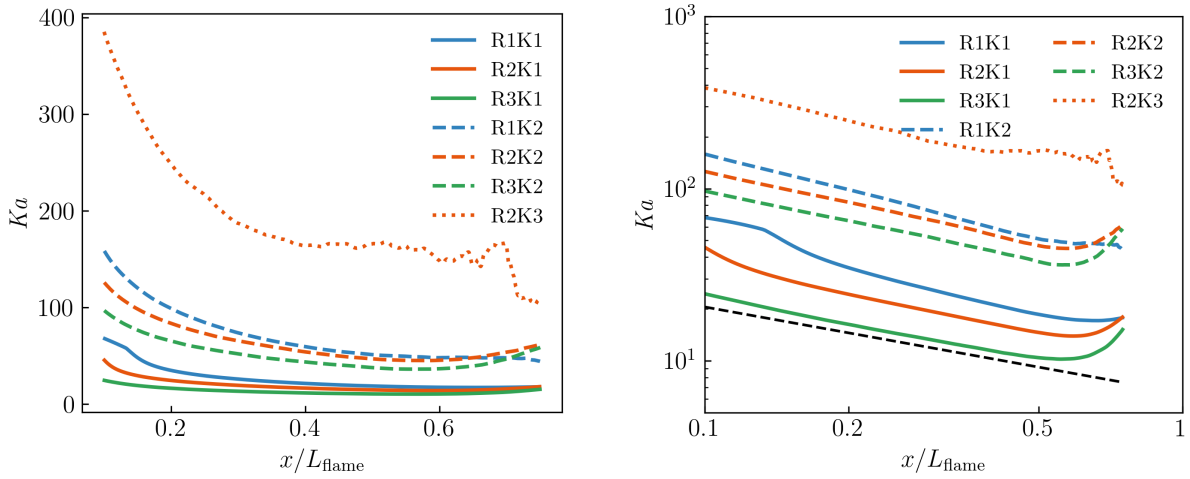

Figure 4: Streamwise evolution of the Karlovitz number Ka for all cases. The black dashed line represents $Ka \propto x^{-0.5}$.

shows the streamwise variation of the Karlovitz number, defined as

$$Ka = \sqrt{\frac{\langle \varepsilon | C_{\mathrm{H_2}} = 0.1 \rangle_s}{\varepsilon_F}}\,, \tag{3}$$

where ε denotes the the turbulent kinetic energy dissipation rate,

$$\varepsilon = \tau_{ij} s_{ij}\,, \tag{4}$$

where τ_{ij} is the viscous stress tensor and s_{ij} is the strain-rate tensor. The operator $\langle \cdot \rangle_s$ represents a surface-weighted ensemble-average evaluated at $C_{\mathrm{H_2}} = 0.1$, and $\varepsilon_F = s_L^3 / l_F$. Note that the Karlovitz number is defined in the unburnt mixture. For all cases, Ka decreases in the streamwise direction due to the decay of dissipation rate. In the center regions of the flame, the power-law relation $Ka \propto x^{-0.5}$ holds approximately.

How to get access to the data

Upon request. Contact the authors:
m.gauding@itv.rwth-aachen.de
lukas.berger@vub.be
h.pitsch@itv.rwth-aachen.de

References

[1] L. Berger, A. Attili, and H. Pitsch. Synergistic interactions of thermodiffusive instabilities and turbulence in lean hydrogen flames. *Combustion and Flame*, 244:112254, 2022.

[2] L. Berger, A. Attili, M. Gauding, and H. Pitsch. Effects of Karlovitz number variations

on thermodiffusive instabilities in lean turbulent hydrogen jet flames. *Proceedings of the Combustion Institute*, 40(1-4):105219, 2024.

[3] R. W. Bilger, S. Stårner, and R. J. Kee. On reduced mechanisms for methane air combustion in nonpremixed flames. *Combustion and Flame*, 80(2):135–149, 1990.

[4] M. P. Burke, M. Chaos, Y. Ju, F. L. Dryer, and S. J. Klippenstein. Comprehensive h2/o2 kinetic model for high-pressure combustion. *International Journal of Chemical Kinetics*, 44 (7):444–474, 2012.

[5] O. Desjardins, G. Blanquart, G. Balarac, and H. Pitsch. High order conservative finite difference scheme for variable density low mach number turbulent flows. *Journal of Computational Physics*, 227(15):7125–7159, 2008.